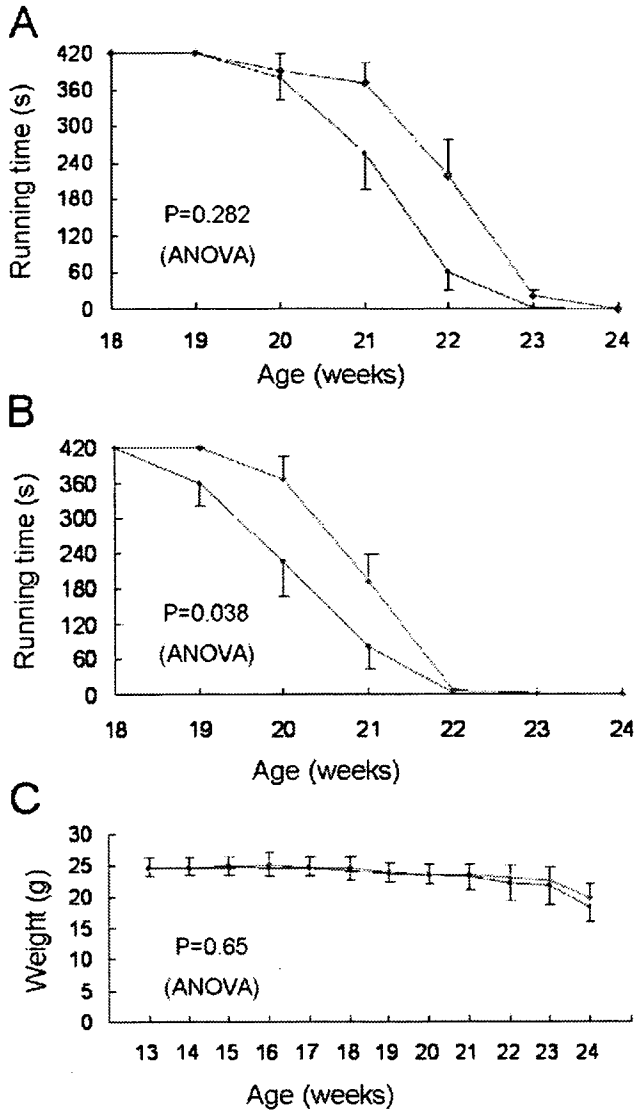

Fig. 4. Motor function of Tg mice (mutant H46R SOD1) tested with the Rotarod. For the 5 rpm task (A), there was no significant difference between the two groups. However, the assessment with the Rotarod task at 20 rpm was much more improved in the gal-1-treated group than in the control group ($P = 0.038$) (B). Red line, gal-1 group ($n = 10$); blue line, control group ($n = 9$). Body weight measurements of the transgenic mice treated with rhGAL-1/ox or physiological saline (C). Red line, gal-1 group ($n = 14$); blue line, control group ($n = 14$). Error bars represent SD.

with those in the gal-1-treated group (18.4 ± 2.4 versus 19.7 ± 2.3 g) (Fig. 4C); however, there was no statistical significance of the body weights between the two groups (ANOVA; $P = 0.65$).

Histopathological evaluation of spinal cords with 147-day-old mice: effect of rhGAL-1/ox on motor neuron survival

In H&E-stained sections, several pathological features were seen in both gal-1-treated group and control group. Neurite swellings, eosinophilic inclusion bodies similar to Lewy body-like hyaline inclusions in human ALS, and astrocytic proliferations were detectable in the anterior horns of the spinal cord. Large anterior horn cells were decreased in number in both groups, however, histological evaluation using Nissl-stained spinal cord sections of the 147-day-old mice suggested a neuroprotective effect of rhGAL-1/ox on spinal motor neuron survival.

In Nissl-stained sections, more anterior horn cells of L_{4-5} segments were preserved in the gal-1-treated group (Fig. 5A) than in the control group (Fig. 5B) ($P = 0.007$, Table 2). Furthermore, we compared the number of remaining large anterior horn cells at the cervical level (C_{5-6}) between the gal-1-treated group and the control group. At the cervical level, gal-1-treated Tg mice also had a greater number of large anterior horn cells than the control group ($P = 0.039$, Table 2). In both the cervical and lumbar spinal cords, there was no significant difference in the number of anterior horn cells between the

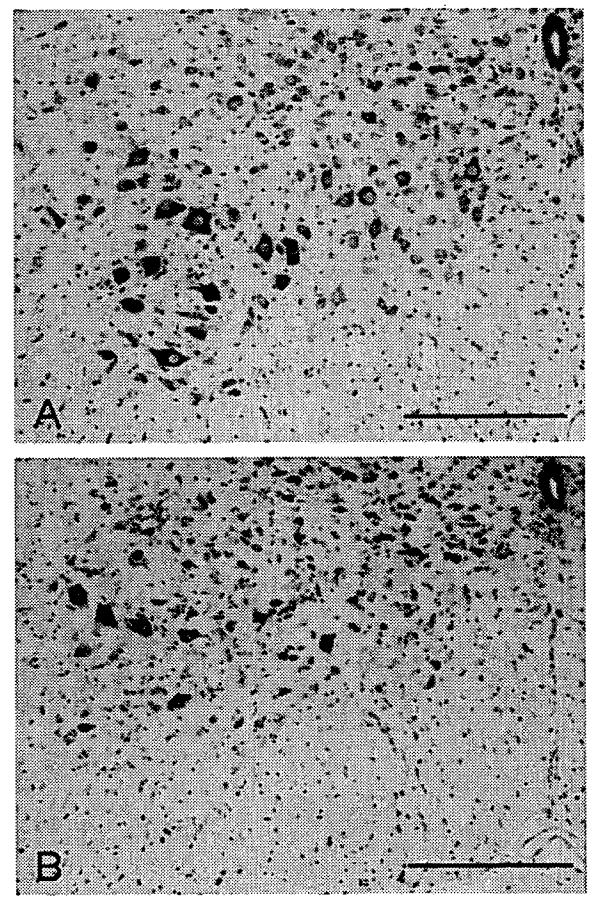

Fig. 5. Histological evaluation of the lumbar cord in 147-day-old mice. (A) rhGAL-1/ox-treated mice, (B) physiological saline-treated mice. In Nissl-stained sections, neuronal cells were well preserved in the anterior horn of the lumbar cord in the gal-1-treated group. Scale bars = 200 μm.

Table 2
The number of large anterior horn neurons/section of spinal cord L_{4-5} and C_{5-6} at postnatal day 147

	n	Lumbar cord		Total	Cervical cord		Total
		L	R		L	R	
Control group	5	3.8 ± 0.3	3.7 ± 0.3	7.5 ± 0.6*	5.7 ± 1.0	5.7 ± 1.1	11.4 ± 2.1*
Gal-1 group	6	6.9 ± 0.8	6.5 ± 0.7	13.5 ± 1.5*	10.0 ± 1.3	10.1 ± 1.6	20.1 ± 2.8*

Values tabulated are mean ± SEM. Statistical comparisons were with a two-tailed Student's *t* test.
n: number of mice examined; R: right side of the spinal cord; L: left side of the spinal cord.
* Gal-1 vs. Control, $P < 0.05$.

injected side (left) and the non-injected side (right) ($P > 0.05$, Table 2).

Discussion

The results of the present study showed the therapeutic effect of rhGAL-1/ox for H46R SOD1 Tg mice, an animal model of FALS. The administration of rhGAL-1/ox prevented the Tg mice from losing spinal anterior horn neurons. In contrast to the control group, rhGAL-1/ox-treated mice showed better behavioral performance and a prolonged life span, consistent with the preservation of spinal motor neurons. In the present study, rhGAL-1/ox was injected into the left gastrocnemius muscle. However, anterior horn cells were well preserved not only in the left side but also in the right side of the anterior horn of the lumbar cord. Moreover, the number of anterior horn cells was well preserved even in the cervical cord. Therefore, it seems that the effect of rhGAL-1/ox on the anterior horn cells is not through retrograde axonal transport.

Galectin-1, a member of the family of β-galactoside-binding lectins, is isolated as a homodimer of the 14.5 kDa subunit. Galectin-1 is present in various tissues and organs, including the lung, heart, skeletal muscle, skin, placenta, thymus, lymph node, brain, spinal cord, and peripheral nerve (Kasai and Hirabayashi, 1996). Several functions for galectin-1 have been proposed in those tissues: cell growth, cell differentiation, apoptosis, cell–cell interaction, and cell–matrix interaction (Perillo et al., 1998).

The galectin-1 molecule has six cysteine residues and, when it is oxidized, three disulfide bonds are formed (Inagaki et al., 2000). An oxidized form of galectin-1 showed axonal regeneration-enhancing activity; however, it lacked a property of lectin to bind to lactose (Inagaki et al., 2000). On the other hand, a reduce form of galectin-1 possessed lectin properties but showed no axonal regeneration-enhancing activity. Indeed, a galectin-1 mutant, in which all six cysteine residues were replaced by serine, induced lectin activity but lacked axonal regeneration-promoting activity (Inagaki et al., 2000).

These three intramolecular disulfide bonds appear to represent a stable conformation of oxidized galectin-1. As these strong covalent linkages are not broken down easily, injected rhGAL-1/ox probably acted as an oxidized form of galectin-1, showing axonal regeneration-enhancing activity. Indeed, rhGAL-1/ox confirmed that the protein promotes axonal regeneration in both in vitro experiments (Horie et al., 2004) and the in vivo acellular nerve regeneration model (Fukaya et al., 2003).

On the other hand, because direct application of oxidized galectin-1 to isolated primary sensory neurons does not alter their morphology, it is hypothesized that galectin-1 may stimulate non-neuronal cells to produce a factor that promotes Schwann cell migration while enhancing axonal regeneration (Horie et al., 1999, 2004). To date, the following issues have been addressed: (1) identification of target cells of galectin-1 among non-neuronal cells surrounding axons and/or neurons; (2) understanding of the mechanism whereby oxidized galectin-1 promotes axonal regeneration.

Recent reports have given possible answers to these questions. The macrophage is one target cell for oxidized galectin-1, and an axonal regeneration-promoting factor is secreted from macrophages stimulated by oxidized galectin-1 in vitro (Horie et al., 2004). Recently, Horie et al. have shown the following results: (1) macrophages bear specific receptors to rhGAL-1/ox on their cell membranes; (2) rhGAL-1 stimulates tyrosine phosphorylation of proteins in macrophages, suggesting that rhGAL-1/ox specifically binds to macrophages to activate their signal transduction pathway; (3) rhGAL-1/ox induces macrophages to secrete a factor(s) to promote axonal regeneration; (4) rhGAL-1/ox stimulates macrophages to enhance Schwann cell migration. Surprisingly, the axonal promoting activity of the conditioned medium secreted from galectin-1-activated macrophages is distinctively stronger than various trophic factors, such as nerve growth factor (NGF), insulin-like growth factor I (IGF-I), insulin-like growth factor II (IGF-II), and ciliary derived neurotrophic factor (CNTF) in vitro (Horie et al., 2004). Further experiments need to be conducted to identify the factor released from rhGAL-1/ox-stimulated macrophages.

To date, the mechanism of motor neuron degeneration in ALS remains unknown; however, several neurotrophic factors (NTFs) or other therapeutic agents have been studied because of their potential ability to protect against motor neuron degeneration. Indeed, these factors have been extensively studied in animal models of ALS. Several agents have shown delay of disease onset and/or survival prolongation, and these agents have been viewed as a new therapeutic strategy for ALS. As for these therapeutic agents,

the mechanisms of action have been considered to be as follows: (1) free radical scavengers (Barneoud and Curet, 1999; Dugan et al., 1997; Gurney et al., 1996); (2) glutamate inhibitors (Gurney et al., 1996); (3) copper chelator (Hottinger et al., 1997); (4) stabilizers of mitochondria (Klivenyi et al., 1999); (5) caspase inhibitors (Li et al., 2000); (6) microglial activation inhibitors (Kriz et al., 2002); and (7) NTFs. At present, riluzole, a glutamate receptor antagonist, is commercially available for patients with ALS (Rowland and Schneider, 2001). As for NTFs, some trials have been performed on patients with ALS; the subcutaneous delivery of IGF-I had marginal success in one of two human trials (Kaspar et al., 2003); however, other NTFs such as the CNTF, the glial cell line-derived neurotrophic factor (GDNF), and the brain-derived neurotrophic factor (BDNF) have been unsuccessful in human trials (Dawbarn and Allen, 2003).

Several investigations have revealed that the impairment of axonal transport is the early event of spinal motor neurons in ALS; disturbance of axonal transport may occur initially and subsequently cause accumulation of neurofilaments in the perikarya and the proximal portion of axons (Collard et al., 1995; Williamson and Cleveland, 1999; Zhang et al., 1997). Impairment of the axonal transport may trap galectin-1 in the perikarya and the proximal portion of the axons of the anterior horn cells in ALS (Kato et al., 2001). It has recently been reported that the axotomy of facial nerve induced transient upregulation of galectin-1 mRNA, suggesting that facial nerve injury can trigger the synthesis of galectin-1 in neuronal cell bodies (Akazawa et al., 2004). Several studies have also shown that galectin-1 is likely to be released from muscle cells and subsequently act as a factor for myogenesis in vivo (Goldring et al., 2002a,b; Gu et al., 1994).

If motor neuron axons and skeletal muscles truly need galectin-1 for their maintenance or survival, depletion of this protein may cause degeneration of the motor neurons and skeletal muscles. Although the mode of action of galectin-1 on spinal motor neurons remains unclear, the results of the present study show a potential therapeutic effect of galectin-1 for patients with ALS.

Acknowledgments

This work was in part supported by The Nakabayashi Trust for ALS Research and a Grant-in-Aid from the Ministry of Education, Science, Sports and Culture of Japan.

References

Akazawa, C., Nakamura, Y., Sango, K., Horie, H., Kohsaka, S., 2004. Distribution of the galectin-1 mRNA in the rat nervous system: its transient upregulation in rat facial motor neurons after facial nerve axotomy. Neuroscience 125, 171–178.

Barneoud, P., Curet, O., 1999. Beneficial effects of lysine acetylsalicylate, a soluble salt of aspirin, on motor performance in a transgenic model of amyotrophic lateral sclerosis. Exp. Neurol. 155, 243–251.

Bruijn, L.I., Houseweart, M.K., Kato, S., Anderson, K.L., Anderson, S.D., Ohama, E., Reaume, A.G., Scott, R.W., Cleveland, D.W., 1998. Aggregation and motor neuron toxicity of an ALS-linked SOD1 mutant independent from wild-type SOD1. Science 281, 1851–1854.

Cleveland, D.W., 1999. From Charcot to SOD1: mechanisms of selective motor neuron death in ALS. Neuron 24, 515–520.

Collard, J.F., Cote, F., Julien, J.P., 1995. Defective axonal transport in a transgenic mouse model of amyotrophic lateral sclerosis. Nature 375, 61–64.

Dawbarn, D., Allen, S.J., 2003. Neurotrophins and neurodegeneration. Neuropathol. Appl. Neurobiol. 29, 211–230.

Dugan, L.L., Turetsky, D.M., Du, C., Lobner, D., Wheeler, M., Almli, C.R., Shen, C.K., Luh, T.Y., Choi, D.W., Lin, T.S., 1997. Carboxyfullerenes as neuroprotective agents. Proc. Natl. Acad. Sci. U. S. A. 94, 9434–9439.

Elroy-Stein, O., Bernstein, Y., Groner, Y., 1986. Overproduction of human Cu/Zn superoxide dismutase in transfected cells: extenuation of paraquat-mediated cytotoxicity and enhancement of lipid peroxidation. EMBO. J. 5, 615–622.

Fukaya, K., Hasegawa, M., Mashitani, T., et al., 2003. Oxidized galectin-1 stimulates the migration of Schwann cells from both proximal and distal stumps of transected nerves and promotes axonal regeneration after peripheral nerve injury. J. Neuropathol. Exp. Neurol. 62, 162–172.

Goldring, K., Jones, G.E., Thiagarajah, R., Watt, D.J., 2002a. The effect of galectin-1 on the differentiation of fibroblasts and myoblasts in vitro. J. Cell Sci. 115, 355–366.

Goldring, K., Jones, G.E., Sewry, C.A., Watt, D.J., 2002b. The muscle-specific marker desmin is expressed in a proportion of human dermal fibroblasts after their exposure to galectin-1. Neuromuscul. Disord. 12, 183–186.

Gu, M., Wang, W., Song, W.K., Cooper, D.N., Kaufman, S.J., 1994. Selective modulation of the interaction of alpha 7 beta 1 integrin with fibronectin and laminin by L-14 lectin during skeletal muscle differentiation. J. Cell Sci. 107, 175–181.

Gurney, M.E., Pu, H., Chiu, A.Y., Dal Canto, M.C., Polchow, C.Y., Alexander, D.D., Caliendo, J., Hentati, A., Kwon, Y.W., Deng, H.X., Chen, W., Zhai, P., Sufit, R.L., Siddique, T., 1994. Motor neuron degeneration in mice that express a human Cu, Zn superoxide dismutase mutation. Science 264, 1772–1775.

Gurney, M.E., Cutting, F.B., Zhai, P., Doble, A., Taylor, C.P., Andrus, P.K., Hall, E.D., 1996. Benefit of vitamin E, riluzole, and gabapentin in a transgenic model of familial amyotrophic lateral sclerosis. Ann. Neurol. 39, 147–157.

Hashimoto-Gotoh, T., Mizuno, T., Ogasahara, Y., Nakagawa, M., 1995. An oligodeoxyribonucleotide-directed dual amber method for site-directed mutagenesis. Gene 152, 271–275.

Hirano, A., Nakano, I., Kurland, L.T., Mulder, D.W., Holley, P.W., Saccomanno, G., 1984. Fine structural study of neurofibrillary changes in a family with amyotrophic lateral sclerosis. J. Neuropathol. Exp. Neurol. 43, 471–480.

Horie, H., Kadoya, T., 2000. Identification of oxidized galectin-1 as an initial repair regulatory factor after axotomy in peripheral nerves. Neurosci. Res. 38, 131–137.

Horie, H., Inagaki, Y., Sohma, Y., Nozawa, R., Okawa, K., Hasegawa, M., Muramatsu, N., Kawano, H., Horie, M., Koyama, H., Sakai, I., Takeshita, K., Kowada, Y., Takano, M., Kadoya, T., 1999. Galectin-1 regulates initial axonal growth in peripheral nerves after axotomy. J. Neurosci. 19, 9964–9974.

Horie, H., Kadoya, T., Hikawa, N., Sango, K., Inoue, H., Takeshita, K., Asawa, R., Hiroi, T., Sato, M., Yoshioka, T., Ishikawa, Y., 2004. Oxidized galectin-1 stimulates macrophages to promote axonal regeneration in peripheral nerves after axotomy. J. Neurosci. 24, 1873–1880.

Hottinger, A.F., Fine, E.G., Gurney, M.E., Zurn, A.D., Aebischer, P., 1997. The copper chelator D-penicillamine delays onset of disease and

extends survival in a transgenic mouse model of familial amyotrophic lateral sclerosis. Eur. J. Neurosci. 9, 1548–1551.

Inagaki, Y., Sohma, Y., Horie, H., Nozawa, R., Kadoya, T., 2000. Oxidized galectin-1 promotes axonal regeneration in peripheral nerves but does not possess lectin properties. Eur. J. Biochem. 267, 2955–2964.

Ioannou, P.A., Amemiya, C.T., Garnes, J., Kroisel, P.M., Shizuya, H., Chen, C., Batzer, M.A., de Jong, P.J., 1994. A new bacteriophage P1-derived vector for the propagation of large human DNA fragments. Nat. Genet. 6, 84–89.

Kadoya, T., Oyanagi, K., Kawakami, E., Hasegawa, M., Inagaki, Y., Sohma, Y., Horie, H., in press. Oxidized galectin-1 advances the functional recovery after peripheral nerve injury. Neurosci. Lett. (Available online in ScienceDirect).

Kasai, K., Hirabayashi, J., 1996. Galectins: a family of animal lectins that decipher glycocodes. J. Biochem. (Tokyo) 119, 1–8.

Kaspar, B.K., Llado, J., Sherkat, N., Rothstein, J.D., Gage, F.H., 2003. Retrograde viral delivery of IGF-1 prolongs survival in a mouse ALS model. Science 301, 839–842.

Kato, T., Kurita, K., Seino, T., Kadoya, T., Horie, H., Wada, M., Kawanami, T., Daimon, M., Hirano, A., 2001. Galectin-1 is a component of neurofilamentous lesions in sporadic and familial amyotrophic lateral sclerosis. Biochem. Biophys. Res. Commun. 282, 166–172.

Klivenyi, P., Ferrante, R.J., Matthews, R.T., Bogdanov, M.B., Klein, A.M., Andreassen, O.A., Mueller, G., Wermer, M., Kaddurah-Daouk, R., Beal, M.F., 1999. Neuroprotective effects of creatine in a transgenic animal model of amyotrophic lateral sclerosis. Nat. Med. 5, 347–350.

Kriz, J., Nguyen, M.D., Julien, J.P., 2002. Minocycline slows disease progression in a mouse model of amyotrophic lateral sclerosis. Neurobiol. Dis. 10, 268–278.

Levanon, D., Lieman-Hurwitz, J., Dafni, N., Wigderson, M., Sherman, L., Bernstein, Y., Laver-Rudich, Z., Danciger, E., Stein, O., Groner, Y., 1985. Architecture and anatomy of the chromosomal locus in human chromosome 21 encoding the Cu/Zn superoxide dismutase. EMBO J. 4, 77–84.

Li, M., Ona, V.O., Guegan, C., Chen, M., Jackson-Lewis, V., Andrews, L.J., Olszewski, A.J., Stieg, P.E., Lee, J.P., Przedborski, S., Friedlander, R.M., 2000. Functional role of caspase-1 and caspase-3 in an ALS transgenic mouse model. Science 288, 335–339.

Manabe, Y., Nagano, I., Gazi, M.S., Murakami, T., Shiote, M., Shoji, M., Kitagawa, H., Abe, K., 2003. Glial cell line-derived neurotrophic factor protein prevents motor neuron loss of transgenic model mice for amyotrophic lateral sclerosis. Neurol. Res. 25, 195–200.

Perillo, N.L., Marcus, M.E., Baum, L.G., 1998. Galectins: versatile modulators of cell adhesion, cell proliferation, and cell death. J. Mol. Med. 76, 402–412.

Ripps, M.E., Huntley, G.W., Hof, P.R., Morrison, J.H., Gordon, J.W., 1995. Transgenic mice expressing an altered murine superoxide dismutase gene provide an animal model of amyotrophic lateral sclerosis. Proc Natl. Acad. Sci. U. S. A. 92, 689–693.

Rowland, L.P., Schneider, N.A., 2001. Amyotrophic lateral sclerosis. N. Engl. J. Med. 344, 1688–1700.

Shefner, J.M., Brown Jr., R.H., Cole, D., Chaturvedi, P., Schoenfeld, D., Pastuszak, K., Matthews, R., Upton-Rice, M., Cudkowicz, M.E., 2001. Effect of neurophilin ligands on motor units in mice with SOD1 ALS mutation. Neurology 57, 1857–1861.

Tu, P.H., Raju, P., Robinson, K.A., Gurney, M.E., Trojanowski, J.Q., Lee, V.M., 1996. Transgenic mice carrying a human mutant superoxide dismutase transgene develop neuronal cytoskeletal pathology resembling human amyotrophic lateral sclerosis lesions. Proc. Natl. Acad. Sci. U. S. A. 93, 3155–3160.

Wang, L.J., Lu, Y.Y., Muramatsu, S., Ikeguchi, K., Fujimoto, K., Okada, T., Mizukami, H., Matsushita, T., Hanazono, Y., Kume, A., Nagatsu, T., Ozawa, K., Nakano, I., 2002. Neuroprotective effects of glial cell line-derived neurotrophic factor mediated by an adeno-associated virus vector in a transgenic animal model of amyotrophic lateral sclerosis. J. Neurosci. 22, 6920–6928.

Warita, H., Itoyama, Y., Abe, K., 1999. Selective impairment of fast anterograde axonal transport in the peripheral nerves of asymptomatic transgenic mice with a G93A mutant SOD1 gene. Brain Res. 819, 120–131.

Williamson, T.L., Cleveland, D.W., 1999. Slowing of axonal transport is a very early event in the toxicity of ALS-linked SOD1 mutants to motor neurons. Nat. Neurosci. 2, 50–56.

Wong, P.C., Pardo, C.A., Borchelt, D.R., Lee, M.K., Copeland, N.G., Jenkins, N.A., Sisodia, S.S., Cleveland, D.W., Price, D.L., 1995. An adverse property of a familial ALS-linked SOD1 mutation causes motor neuron disease characterized by vacuolar degeneration of mitochondria. Neuron 14, 1105–1116.

Zhang, B., Tu, P., Abtahian, F., Trojanowski, J.Q., Lee, V.M., 1997. Neurofilaments and orthograde transport are reduced in ventral root axons of transgenic mice that express human SOD1 with a G93A mutation. J. Cell Biol. 139, 1307–1315.

HIGH LIGHT

Rapid disease progression correlates with instability of mutant *SOD1* in familial ALS

Abstract—Studies on the clinical course of familial ALS suggest that the duration of illness is relatively consistent for each mutation but variable among the different mutations. The authors analyzed the relative amount of mutant compared with normal SOD1 protein in the erythrocytes from 29 patients with ALS with 22 different mutations. Turnover of mutant SOD1 correlated with a shorter disease survival time.

NEUROLOGY 2005;65:1954–1957

T. Sato, MD*; T. Nakanishi, PhD*; Y. Yamamoto, MD, PhD; P.M. Andersen, MD, PhD; Y. Ogawa, MD, PhD; K. Fukada, MD, PhD; Z. Zhou, MD, PhD; F. Aoike, MD; F. Sugai, MD; S. Nagano, MD, PhD; S. Hirata, MD; M. Ogawa, MD, PhD; R. Nakano, MD, PhD; T. Ohi, MD, PhD; T. Kato, MD, PhD; M. Nakagawa, MD; T. Hamasaki, PhD; A. Shimizu, MD, PhD; and S. Sakoda, MD, PhD

One hundred fourteen different mutations have been reported in the Cu/Zn superoxide dismutase (*SOD1*) gene. The age at onset varies greatly among patients with ALS with a given mutation, but the duration of illness seems to be relatively consistent for a given mutation.[1,2] Therefore, the duration of illness is considered to be closely linked to some property of each mutant protein.

We devised a simple method to distinguish mutant SOD1 protein from normal SOD1 protein using liquid chromatography electrospray ionization mass spectrometry (LC-ESI-MS).[3] We found that the ratio of mutant/normal SOD1 protein was 0.60 in the diaphragm, 0.47 in the iliopsoas muscle, 0.43 in the spinal cord, and 0.14 in erythrocytes for the His46Arg mutant.[4] Because no protein synthesis occurs in the enucleated erythrocytes and the average cell age is 60 days, the instability of mutant SOD1 should be more apparent in erythrocytes compared with most other cells in the body.

We performed a systematic analysis of the relative amount of human mutant SOD1 proteins in erythrocytes in relation to the clinical course of ALS with 22 different *SOD1* gene mutations.

Methods. ALS was diagnosed according to the revised El Escorial criteria of the World Federation of Neurology. With informed consent, *SOD1* gene[2] and protein studies[3] were performed. The age at onset is the time of the first sign of muscle weakness, atrophy, or clinical symptoms involving upper or lower motor neurons. The duration of illness is the period from onset to respiratory failure. The protein analysis has been described.[3] The combined data from both dead and living patients were analyzed by log-normal regression using the EM algorithm, with the duration of illness as a response, and the ratio and age at onset as covariates.

Results. The *SOD1* gene and protein in erythrocytes of 29 patients with ALS and four carriers were analyzed by genomic sequencing and LC-ESI-MS. Twenty-seven patients presented with muscle weakness in their extremities, and 2 patients noticed dyspnea as the initial symptom of ALS. As representative data, transformed mass spectra of SOD1 protein from Patients 23 and 25 are shown in figure 1. The molecular masses of the peaks in figure 1, A and B, were 15846.2 Da and 15845.0 Da, which coincided with the theoretical average for the monomer of normal SOD1, 15844.6 Da. SOD1 from Patient 23 showed an ion peak of mutant SOD1 in addition to a normal peak (see figure 1A). The mutant peak had a molecular mass of 15820.7 Da, and the difference of 25.5 Da corresponded to the mutation from leucine to serine. In Patient 25, we could not detect any significant peaks except the normal peak (see figure 1B). We measured the intensities of the signals for SOD1 and mutant SOD1, and the results are shown in the table. The samples from Patients 14 and 15, whose ratios of mutant/normal SOD1 were 0.50 and 0.57, respectively, had been stored at −80 °C for 15 months and 5 years. Similarly, those from

This article was previously published in electronic format as an Expedited E-Pub on November 16, 2005, at www.neurology.org.

* These authors contributed equally to this work.

From the Department of Neurology (Drs. Sato, Yamamoto, Y. Ogawa, Fukada, Zhou, Aoike, Sugai, Nagano, and Sakoda), Department of Medical Statistics (Dr. Hamasaki), Osaka University Graduate School of Medicine, Suita, Osaka, Japan; Department of Clinical Pathology (Drs. Nakanishi and Shimizu), Osaka Medical College, Takatsuki, Osaka, Japan; Awaji Prefectural Hospital (Dr. Hirata), Sumoto, Hyogo, Japan; Aomori Prefectural Central Hospital (Dr. M. Ogawa), Aomori, Japan; Department of Neurology (Dr. Nakano), Brain Research Institute, Niigata University, Niigata, Japan; Division of Neurology (Dr. Ohi), Department of Internal Medicine, Miyazaki University School of Medicine, Miyazaki, Japan; Third Department of Internal Medicine (Dr. Kato), Yamagata University School of Medicine, Yamagata, Japan; Department of Neurology and Gerontology (Dr. Nakagawa), Research Institute for Neurological Diseases and Geriatrics, Kyoto Prefectural University of Medicine, Kyoto, Japan; and Department of Neurology (Dr. Andersen), Umeå University Hospital, Umeå, Sweden.

Supported by Grants-in-Aid for Scientific Research in Japan and by a grant on Specific Diseases (Y.I.) from the Ministry of Health and Welfare, Japan.

Disclosure: The authors report no conflicts of interest.

Received August 4, 2004. Accepted in final form September 1, 2005.

Address correspondence and reprint requests to Dr. Yoichi Yamamoto, Department of Neurology D4, Osaka University Graduate School of Medicine, 2-2 Yamada-oka, Suita, Osaka 565-0871, Japan; e-mail: yamamoto@neurol.med.osaka-u.ac.jp

Editorial, see page 1859

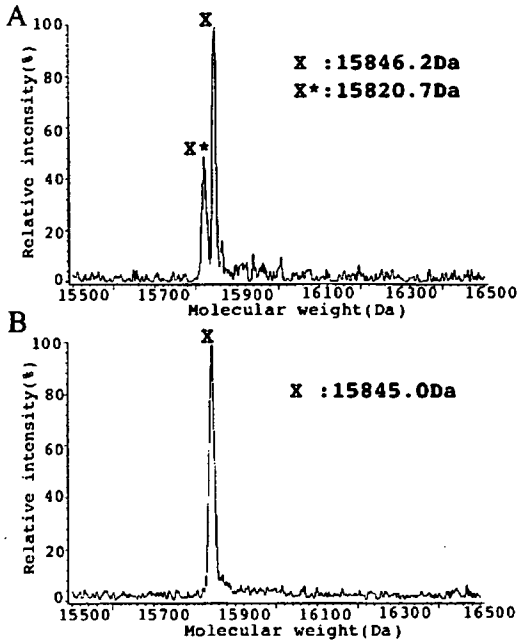

Figure 1. Transformed electrospray ionization (ESI) mass spectra of SOD1 prepared by immunoprecipitation from Patient 23 (A) and Patient 25 (B) listed in the table. X and X indicate normal and mutant monomer SOD1, respectively.*

Patients 33 and 18, whose ratios were 0.34 and 0.29, respectively, had been stored for 29 months and 5.6 years. These results indicated that the duration of preservation had little effect on the ratio. The ratios from three patients and two carriers with the Ala4Val mutation were not detected.

First, we found that the age at onset and the duration of illness were independent of each other ($p = 0.7157$). Next, we plotted the ratio of mutant/normal SOD1 against age at disease onset (figure 2A) or duration of illness (figure 2B). We found that the age at onset had no relationship with the ratio. Conversely, to assess the effects of covariates on the duration of illness, we performed the likelihood ratio test, and found that the effect of this ratio on the duration of illness was evident at the level of 5% ($p = 0.0029$; see figure 2B). In addition, to examine whether the survival time of the patient was longer or shorter if the ratio was greater or less than a certain value, the values of the Akaike Information Criterion (AIC), an index commonly used as an aid for choosing between competing models, were computed,[5] categorizing the value of the ratio into two groups. The value of AIC was the smallest when categorizing the ratio into two groups, not detected and detected (AIC = −55.312), and this suggests that the difference in the duration of illness is the largest between

Table *Summary of clinical features and mutant/normal SOD1*

Case	Sex	SOD1 mutation	Age at onset, y	Site of onset	Duration of illness	Mutant/normal SOD1
1	M	Ala4Ser	34	L leg	>3 y	0.56
2	M	Ala4Thr	21	L lower limb	20 mo	Not detected
3	M	Ala4Val	43	R hand	32 mo	Not detected
4	M	Ala4Val	60	R hand	7 mo	Not detected
5	F	Ala4Val	48	L arm	14 mo	Not detected
6	M	Val14Gly	41	Leg paresis	20 mo	0.33
7	M	Gly37Arg	41	R hand	6 y	0.56
8	M	Gly41Asp	36	R leg	>11 y	Not detected
9	F	His46Arg	59	R lower limb	5 y	0.11
10	M	His46Arg	46	L lower limb	>11 y	0.18
11	M	Asp76Tyr	49	R foot	17 y	0.61
12	F	Asn86Ser	36	L leg	9 y	0.12
13	M	Asn86Ser	63	R foot	6 y	0.12
14	M	Ala89Val	70	R foot	>35 mo	0.5
15	F	Ala89Val	55	L foot	>6 y	0.57
16	M	Asp101His	52	R hand	3 mo	Not detected
17	F	Ser105Leu	54	R arm	5 y	Not detected
18	F	Ile113Thr	63	L arm	19 mo	0.29
19	F	Ile113Phe	68	L leg	>6 y	0.23
20	M	Gly114Ala	38	L hand	29 mo	Not detected
21	M	Arg115Gly	66	L leg	>22 mo	Not detected
22	F	Leu1262bp del	42	R foot	17 mo	Not detected
23	M	Leu126Ser	63	Bilateral feet	>3 y	0.5
24	M	Gly127insTGGG	52	Bulbar	8 mo	Not detected
25	M	Ser134Asn	52	R upper limb	9 mo	Not detected
26	M	Ser134Asn	39	Bulbar	10 mo	Not detected
27	M	Gly141Glu	43	R leg	> 4 y	0.28
28	M	Leu144Phe	71	R leg	>12 mo	0.29
29	F	Leu144Phe	42	L foot	>3 y	0.29
30	M	Ala4Val	Unaffected			Not detected
31	F	Ala4Val	Unaffected			Not detected
32	F	Asp76Tyr	Unaffected			0.58
33	M	Ile113Thr	Unaffected			0.34

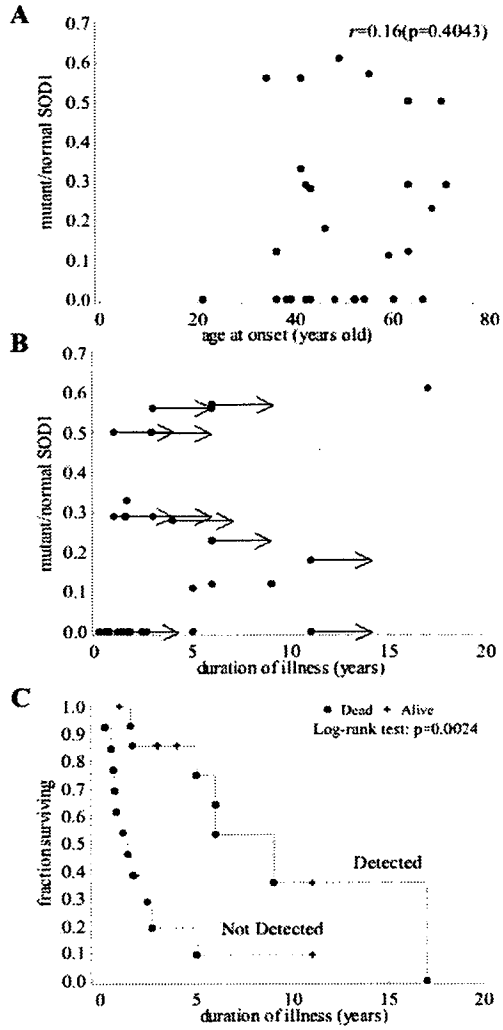

Figure 2. Ratio of mutant/normal SOD1 protein in erythrocytes plotted against clinical course. Ratio 0 indicates mutant protein was not detected. (A) Age at onset. (B) Duration of illness. Arrows designate that patients are alive. (C) Kaplan–Meier survival curve plot. Filled circles represent dead patients, and crosses represent living patients. Solid line and dashed line represent mutant SOD1 proteins that were detected or not detected, respectively. The median survival time was estimated as 1.4 years (95% CI 0.8 to 11.0 years) for the not-detected group and 9.0 years (95% CI 6.0 to 17.0 years) for the detected group. This curve shows that the survival curve for the detected group is always higher than that for the not-detected group. This means that patients in the detected group are alive longer than those in the not-detected group. The two groups did not contain the same type of mutation.

these two groups, as shown by the Kaplan–Meier survival curve plot (figure 2C).

Discussion. The stability of SOD1 mutant protein has been investigated using in vitro models. Unfolding transitions of purified SOD1 mutant holoproteins and apoproteins were examined. The results showed that patients with severe loss of stability of apo-SOD1 have a low mean survival time.[6] Based on the half-lives of the proteins estimated using transfection of plasmids encoding wild-type or mutant SOD1 into cell lines, it was reported that clinical progression was not correlated with the half-lives of the mutant SOD1 proteins.[7]

In mice transgenic for the Gly93Ala and Gly37Arg SOD1 mutations, a high copy number of the mutant *SOD1* gene was required for the development of motor neuron disease, indicating that a large amount of mutant SOD1 protein is necessary for the disease expression in these models. Conversely, in transgenic mice carrying Gly85Arg or Gly127insTGGG SOD1 and showing extremely rapid disease progression, the mutant protein was not detectable in erythrocytes and was barely detected in spinal cord extracts.[8,9] Using highly specific antibodies against the truncated Gly127insTGGG SOD1 mutant, it was shown that the amount of mutant SOD1 protein was less than 0.5% of that of the normal SOD1 protein in the brain and spinal cord of the patient. In addition, the immunohistopathologic study of the spinal cord of the patient revealed that motor neuron inclusions were labeled by antibody directed against ubiquitin and some were also labeled by the mutant-specific antibody. These results suggest that at least part of the SOD1 was degraded via a ubiquitin-dependent pathway.[9]

We previously classified SOD1 mutants into stable type (detected group in this study) and unstable type (not-detected group in this study).[10] The transgenic mice carrying stable-type SOD1 mutations (Gly93Ala and Gly37Arg) were reported to show vacuolation pathology, and those carrying unstable-type mutations (Gly85Arg and Gly127insTGGG) had Lewy body–like inclusions in motor neurons and astrocytes. Therefore, the stability of the SOD1 mutant proteins is deeply involved in not only the clinical course but also the pathology of familial ALS.

The not-detected group included an American patient with the Gly41Asp mutation who is currently alive with disease duration of 11 years. This indicates that although the stability of the mutant protein correlates well with the disease progression statistically, there might be other factors influencing the disease duration, at least for the Gly41Asp mutation. We analyzed erythrocytes from three patients and two carriers with the Ala4Val mutation, and the mutant protein was not detected in any of them. We also analyzed samples from one patient and one carrier each with the Asp76Tyr or Ile113Thr mutation and found that the ratios were 0.61 and 0.58 for the Asp76Tyr mutation or 0.29 and 0.34 for the Ile113Thr mutation (see table). Although the function of the synthesis and degradation of each mutant protein throughout life is still unknown, these results indicate that the ratio may not change during the course of the disease. Whether molecules that stabilize the unstable mutants could be useful for therapy for familial ALS remains to be tested.

References

1. Radunovic A, Leigh PN. Cu/Zn superoxide dismutase gene mutations in amyotrophic lateral sclerosis: correlation between genotype and clinical features. J Neurol Neurosurg Psychiatry 1996;61:565–572.
2. Andersen PM, Nilsson P, Keranen ML, et al. Phenotypic heterogeneity in motor neuron disease patients with CuZn-superoxide dismutase mutations in Scandinavia. Brain 1997;120:1723–1737.
3. Nakanishi T, Kishikawa M, Miyazaki A, et al. Simple and defined method to detect the SOD-1 mutants from patients with familial amyotrophic lateral sclerosis by mass spectrometry. J Neurosci Methods 1998;81:41–44.
4. Arisato T, Okubo R, Arata H, et al. Clinical and pathological studies of familial amyotrophic lateral sclerosis (FALS) with SOD1 H46R mutation in large Japanese families. Acta Neuropathol (Berl) 2003;106:561–568.
5. Akaike H. Information theory and an extension of the maximum likelihood principle. In: Petrov BN, Csaki F, eds. The 2nd International Symposium on Information Theory. Budapest, Akademi Kaido, 1972: 267–281.
6. Lindberg MJ, Tibell L, Oliveberg M. Common denominator of Cu/Zn superoxide dismutase mutants associated with amyotrophic lateral sclerosis: decreased stability of the apo state. Proc Natl Acad Sci USA 2002;99:16607–16612.
7. Ratovitski T, Corson LB, Strain J, et al. Variation in the biochemical/biophysical properties of mutant superoxide dismutase 1 enzymes and the rate of disease progression in familial amyotrophic lateral sclerosis kindreds. Hum Mol Genet 1999;8:1451–1460.
8. Bruijn LI, Becher MW, Lee MK, et al. ALS-linked SOD1 mutant G85R mediates damage to astrocytes and promotes rapidly progressive disease with SOD1-containing inclusions. Neuron 1997;18:327–338.
9. Jonsson PA, Ernhill K, Andersen PM, et al. Minute quantities of misfolded mutant superoxide dismutase-1 cause amyotrophic lateral sclerosis. Brain 2004;127:73–88.
10. Fukada K, Nagano S, Satoh M, et al. Stabilization of mutant Cu/Zn superoxide dismutase (SOD1) protein by coexpressed wild SOD1 protein accelerates the disease progression in familial amyotrophic lateral sclerosis mice. Eur J Neurosci 2001;14:2032–2036.

Rapid disease progression correlates with instability of mutant SOD1 in familial ALS

T. Sato, T. Nakanishi, Y. Yamamoto, P. M. Andersen, Y. Ogawa, K. Fukada, Z. Zhou, F. Aoike, F. Sugai, S. Nagano, S. Hirata, M. Ogawa, R. Nakano, T. Ohi, T. Kato, M. Nakagawa, T. Hamasaki, A. Shimizu and S. Sakoda

Neurology 2005;65;1954-1957; originally published online Nov 16, 2005;
DOI: 10.1212/01.wnl.0000188760.53922.05

Journal of Neuroscience Research 85:395–401 (2007)

Role of p53 in Neurotoxicity Induced by the Endoplasmic Reticulum Stress Agent Tunicamycin in Organotypic Slice Cultures of Rat Spinal Cord

Jun Tashiro,[1]* Seiji Kikuchi,[1] Kazuyoshi Shinpo,[2] Riichiro Kishimoto,[1] Sachiko Tsuji,[1] and Hidenao Sasaki[1]

[1]Department of Neurology, Hokkaido University Graduate School of Medicine, Kita-ku, Sapporo, Hokkaido, Japan
[2]Nishimaruyama Hospital, Chuo-ku, Sapporo, Hokkaido, Japan

The endoplasmic reticulum (ER) is important for maintaining the quality of cellular proteins. Various stimuli can disrupt ER homeostasis and cause the accumulation of unfolded or misfolded proteins, i.e., a state of ER stress. Recently, ER stress has been reported to play an important role in the pathogenesis of neurological disorders such as cerebral ischemia and neurodegenerative diseases, but its involvement in the spinal cord diseases has not been fully discussed. We conducted this study using tunicamycin (Tm) as an ER stress inducer for rat spinal cord in organotypic slice culture, a system that we have recently established. Tm was shown to induce ER stress by increased expression of GRP78. The viability rate of spinal cord neurons decreased in a dose-dependent manner with Tm treatment, and dorsal horn interneurons were more vulnerable to Tm-induced neurotoxicity. A p53 inhibitor significantly increased the viability of dorsal horn interneurons, and immunofluorescence studies showed nuclear accumulation of p53 in the dorsal horns of Tm-treated spinal cord slices. These findings suggest that p53 plays an important role in the killing of dorsal horn interneurons by Tm. In contrast, motor neurons were not protected by the p53 inhibitor, suggesting that the role of p53 may vary between different cell types. This difference might be a clue to the mechanism of the stress-response pathway and might also contribute to the potential application of p53 inhibitors for the treatment of spinal cord diseases, including amyotrophic lateral sclerosis.

Key words: endoplasmic reticulum; unfolded protein response; dorsal horn interneuron; pifithrin-α

The endoplasmic reticulum (ER) is an intracellular organelle that is important for the folding and maturation of transmembrane and secretory proteins (Liu and Kaufman, 2003). The ER is highly sensitive to alterations of cellular homeostasis and provides strict quality control to ensure that only correctly folded proteins are transported to the Golgi apparatus. A number of biochemical and physiologic stimuli can disrupt ER homeostasis and cause the intraluminal accumulation of unfolded or misfolded proteins, when cells activate a signaling pathway called *unfolded protein response* (UPR; Zhang and Kaufman, 2006). The UPR includes induction of the transcription of UPR genes, a translational attenuation of global protein synthesis, and ER-associated degradation (Liu and Kaufman, 2003). If cells fail to cope with the adverse stimuli by these responses, apoptosis is inevitable.

Recently, ER stress has been reported to play an important role in the pathogenesis of a wide variety of neurological conditions (Shen et al., 2004; Paschen and Mengesdorf, 2005), such as cerebral ischemia (DeGracia and Montie, 2004), and neurodegenerative diseases, including Alzheimer's disease (Katayama et al., 2004) and Parkinson's disease (Paschen and Frandsen, 2001; Takahashi et al., 2003; Takahashi and Imai, 2003; Kheradpezhouh et al., 2003), and polyglutamine diseases (Nishitoh et al., 2002) as well as prion diseases (Hetz et al., 2003), Pelizaeus-Merzbacher disease (Swanton et al., 2005), GM1 gangliosidosis (Tessitore et al., 2004), and inclusion body myositis (Vattemi et al., 2004). However, most experiments reported so far have involved cell lines, and only a few studies have used spinal cord cells to assess the pathogenesis of spinal cord disease

Contract grant sponsor: Research Committee for CNS Degenerative Disease and Group Research in the Pathogenesis and Pathomechanism of Amyotrophic Lateral Sclerosis, Ministry of Health, Labor and Welfare of Japan.

*Correspondence to: Jun Tashiro, Department of Neurology, Hokkaido University Graduate School of Medicine, Kita-15 Nishi-7 Kita-ku, Sapporo, Hokkaido, 060-8638 Japan. E-mail: jtashiro@med.hokudai.ac.jp

Received 19 April 2006; Revised 18 August 2006; Accepted 16 September 2006

Published online 27 November 2006 in Wiley InterScience (www.interscience.wiley.com). DOI: 10.1002/jnr.21120

from the perspective of ER stress (Tobisawa et al., 2003; Wootz et al., 2004).

Amyotrophic lateral sclerosis (ALS) is a neurodegenerative disease that selectively affects the upper and lower motor neurons. Most ALS cases are sporadic, but approximately 10% are familial. Among the familial patients, about 20% have mutations of the gene encoding Cu/Zn superoxide dismutase (SOD1; Rosen et al., 1993; Hervias et al., 2005). Mutations of the SOD1 gene and the associated mechanisms leading to neuronal death such as mitochondrial dysfunction (Hervias et al., 2005), fragmentation of the Golgi apparatus (Fujita and Okamoto, 2005), and activation of caspases (Wootz et al., 2004) have been discussed extensively, but the contribution of ER stress has not yet been fully elucidated (Tobisawa et al., 2003).

We have been investigating the mechanisms of neuronal damage in the spinal cord. Our previous studies were focused on dysfunction of the ubiquitin-proteasome system (Kikuchi et al., 2002), ER stress (Kikuchi et al., 2003), and the related effector pathways. In these two studies, we used lactacystin and epoxomicin as proteasome inhibitors and brefeldin A (BFA) as the ER stress inducer, in a dissociated culture system, and the results of both studies suggested that motor neurons were more vulnerable to the toxicity of those agents than nonmotor neurons.

More recently, we established an organotypic slice culture method for rat spinal cord that makes it easier to identify each cell type accurately, because the architecture of the spinal cord is preserved in the transverse plane (Tsuji et al., 2005). By using this method, we evaluated the effect of proteasome inhibition on rat spinal cord neurons, and selective toxicity for motor neurons was clearly demonstrated. To evaluate further the effects of ER stress on spinal cord neurons, we conducted the present study with another ER stress inducer, tunicamycin (Tm), and the organotypic slice culture system. In addition, studies with p53 inhibitor were performed to investigate the role of p53 in the pathways leading to neuronal death.

MATERIALS AND METHODS

All procedures were performed in accordance with the Guide for the Care and Use of Laboratory Animals, Hokkaido University Graduate School of Medicine.

Materials

The drugs and reagents used in our experiments were as follows: SMI-32 (Sternberger Monoclonals Incorporated, Lutherville, MD), anti-calretinin antibody (Chemicon, Temecula, CA), anti-p53 monoclonal antibody (BD-Biosciences, San Jose, CA), anti-p53 polyclonal antibody (Santa Cruz Biotechnology, Santa Cruz, CA), anti-glucose-regulated protein (GRP) 78 antibody (StressGen Biotechnologies, San Diego, CA), anti-β-actin antibody (Sigma, St. Louis, MO), peroxidase anti-mouse IgG (H + L) and anti-rabbit IgG antibodies (Vector, Burlingame, CA), Alexa Flour 488 goat anti-mouse IgG and Alexa Flour 568 goat anti-rabbit IgG antibodies (Molecular Probes, Eugene, OR), Eagle's minimum essential medium and glutamine (Nissui, Tokyo, Japan), fetal bovine serum and Gey's balanced solution (Sigma), Hank's balanced salt solution (Gibco BRL, Grand Island, NY), brefeldin A and tunicamycin (Sigma); pifithrin-α (Calbiochem, San Diego, CA), and Hoechst 33258 (Sigma).

Organotypic Slice Culture

Organotypic slice cultures were prepared as described previously (Tsuji et al., 2005). Under deep anesthesia with ketamine, neonatal Sprague-Dawley rats on the day 7 were euthanized by decapitation, and their lumbar spinal cords were removed. Nerve roots and excess connective tissue were removed in cooled Gey's balanced salt solution containing 6.5 mg/ml glucose. Then, the spinal cords were cut into 400-μm slices with a McIlwain tissue chopper (Mickle Laboratory Engineering, Gomshall, Surrey, United Kingdom). Four or five slices were set on a membrane insert (Millicell-CM, Millipore, Bedford, MA) and placed into a six-well culture dish with 1 ml of culture medium consisting of 50% Eagle's minimum essential medium, 25% Hank's balanced salt solution, 25% horse serum, 6.4 mg/ml glucose, and 2 mM l-glutamine. The slices were incubated at 37°C in a 5% CO_2 incubator, and the culture medium was changed twice per week. All cultures were used in the experiments after 10 days in vitro.

Experimental Treatment

The spinal cord slices were exposed to Tm at various concentrations (1–20 μg/ml) and BFA at 50 μM on the tenth day of culture. Slices were incubated for about 24 hr before performing Western blot analysis and for about 72 hr before Western blotting and immunohistochemistry or immunofluorescence in a 5% CO_2 incubator maintained at 37°C. To study the protective effect against Tm-induced toxicity, a synthetic inhibitor of p53 [pifithrin-α (PFT)] was added to the culture medium simultaneously with Tm. All reagents added to the culture medium were diluted in dimethyl sulfoxide, and the final concentration of dimethyl sulfoxide was adjusted to be identical in each well, including the control.

Western Blot Analysis

After slices had been incubated for about 24 and 72 hr, they were rinsed with phosphate-buffered saline (PBS) and then homogenized in a sample buffer containing 2 mM EDTA, 2.3% sodium dodecyl sulfate (SDS), 10% glycerol, and 62.5 mM Tris (pH 6.9). After centrifugation at 15,000 rpm for 15 min, the supernatant was stored frozen at −20°C. Proteins were separated by SDS-polyacrylamide gel electrophoresis (10% acrylamide) and transferred electrophoretically to a nitrocellulose membrane. Blots were incubated with the primary antibody and subsequently with the secondary antibody, followed by development with an ECL kit (Amersham, Piscataway, NJ). Anti-GRP78 antibody (1:20,000) and anti-β-actin antibody (1:5,000) were used as the primary antibodies. The density of each band was measured with Image J software (National Institutes of Health, Bethesda, MD), and the relative band intensity was obtained as the density of Tm-treated band

divided by that of control band of each experiment after the adjustment by using corresponding density of β-actin band.

Immunohistochemistry and Immunofluorescence

For labeling of neurons in the spinal cord slices, cultures were fixed with 4% paraformaldehyde for 1 hr; rinsed with PBS; and, after blocking, stained overnight at 4°C with SMI-32 (1:2,500) or anti-calretinin antibody (1:5,000) diluted in PBS containing 0.3% Triton X-100 and 0.2% bovine serum albumin. After several washes with PBS containing 0.3% Triton X-100, the slices were incubated with secondary antibodies (1:250) for 5 hr and then visualized with diaminobenzidine tetrahydrochloride (DAB).

For immunofluorescence, the fixation procedure and primary antibodies were the same as described above, except that the two primary antibodies were used together for double staining. Incubation with the secondary antibodies (1:100), Alexa Flour 488 goat anti-mouse IgG and Alexa Flour 568 goat anti-rabbit IgG, was for 1 hr. Photographs were taken with a fluoroscope with a CCD camera (Nikon, Tokyo, Japan) and were colored with imaging software or were taken by using a confocal microscope (MRC-1024; Bio-Rad).

Definition of Viable Neurons and Statistical Analysis

Organotypic slice culture has the advantage of allowing both immunoreactivity and anatomical location to be assessed for accurate identification of cells. We defined viable motor neurons as SMI-32-positive cells with a large cell body (>30 μm) located in the anterior horn of the spinal cord, whereas dorsal horn interneurons were defined as anti-calretinin antibody-positive cells in the dorsal horn.

We counted the number of viable motor neurons and dorsal horn interneurons in each slice. The average number of viable cells in each slice was calculated, and the viability rate was obtained as the average number under each test condition divided by that in the control for every experiment. The experiments were repeated at least three times independently. Statistical analysis was perfomed by using the Kruskal-Wallis test, Welch's *t*-test, and Student's *t*-test with Microsoft Excel add-in software (Statcel 2).

RESULTS

Induction of ER Stress by Tm in Organotypic Slice Culture

Western blot analysis showed increased expression of GRP78 in slices incubated with 2 μg/ml Tm for 24 hr compared with control slices, and, even after 72-hr incubation with 1 μg/ml Tm, the increased expression of GRP78 persisted (Fig. 1). The GRP proteins are constitutively expressed in all cells, and their transcription is induced by a number of different stimuli that disrupt ER function (Kaufman, 1999). Among these proteins, GRP78 is the best characterized ER-stress marker and ER molecular chaperone, and it serves as a master regulator that plays an essential role in activating important transducers for initiation of the UPR (Zhang and Kaufman, 2006). Thus, this finding suggests that exposure to Tm caused ER stress in cultured slices of rat spinal cord.

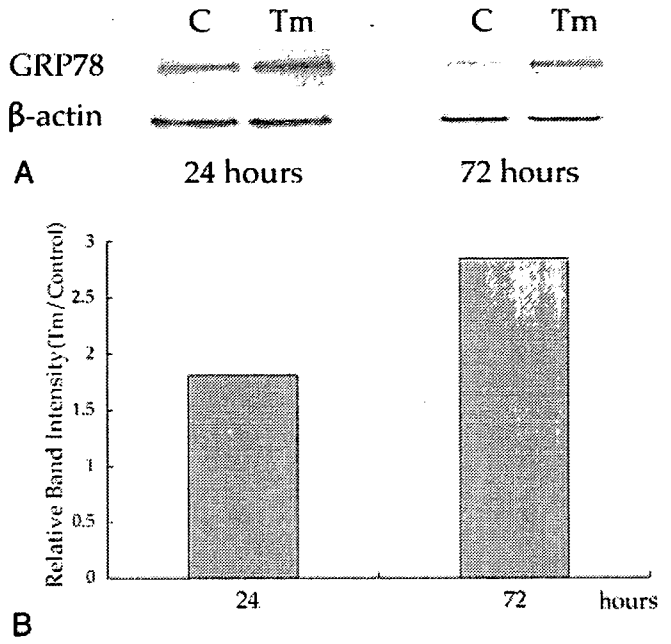

Fig. 1. Western blots showing increased expression of GRP78 in the Tm-treated group after 24 and 72 hr of incubation (**A**). Relative band intensity calculated from the densities of bands measured in Western blots (**B**). Increased GRP78 expression was shown to persist even after 72 hr of incubation. Tm, tunicamycin; C, control.

Toxicity of Tm for Spinal Cord Neurons

The viability rate of both motor neurons and dorsal horn interneurons decreased in a dose-dependent manner (Fig. 2), indicating that Tm was toxic for spinal cord neurons in organotypic slice culture. In addition, the viability rate of dorsal horn interneurons was considerably lower than that of motor neurons at the low concentration of Tm. These results suggest that dorsal horn interneurons were more highly susceptible to Tm-induced neurotoxicity.

Differing Effects of BFA and Tm on Spinal Cord Neurons

Although the number of slices was not sufficient for statistical analysis, motor neurons were more severely damaged than dorsal horn interneurons in BFA-treated slices (Fig. 2). This finding is consistent with the results of our previous study, which showed that motor neurons were more vulnerable to BFA-induced neurotoxicity in dissociated culture (Kikuchi et al., 2002). Both Tm and BFA are ER stress inducers, but they showed different profiles of spinal cord neuronal damage.

Protective Effect of PFT on Spinal Neurons Against Tm-Induced Neurotoxicity

When the slices were incubated concomitantly with Tm and PFT, a p53 inhibitor, the viability rate of dorsal horn interneurons showed a significant increase at 1, 2, and 10 μg/ml of Tm (Fig. 3), except when the

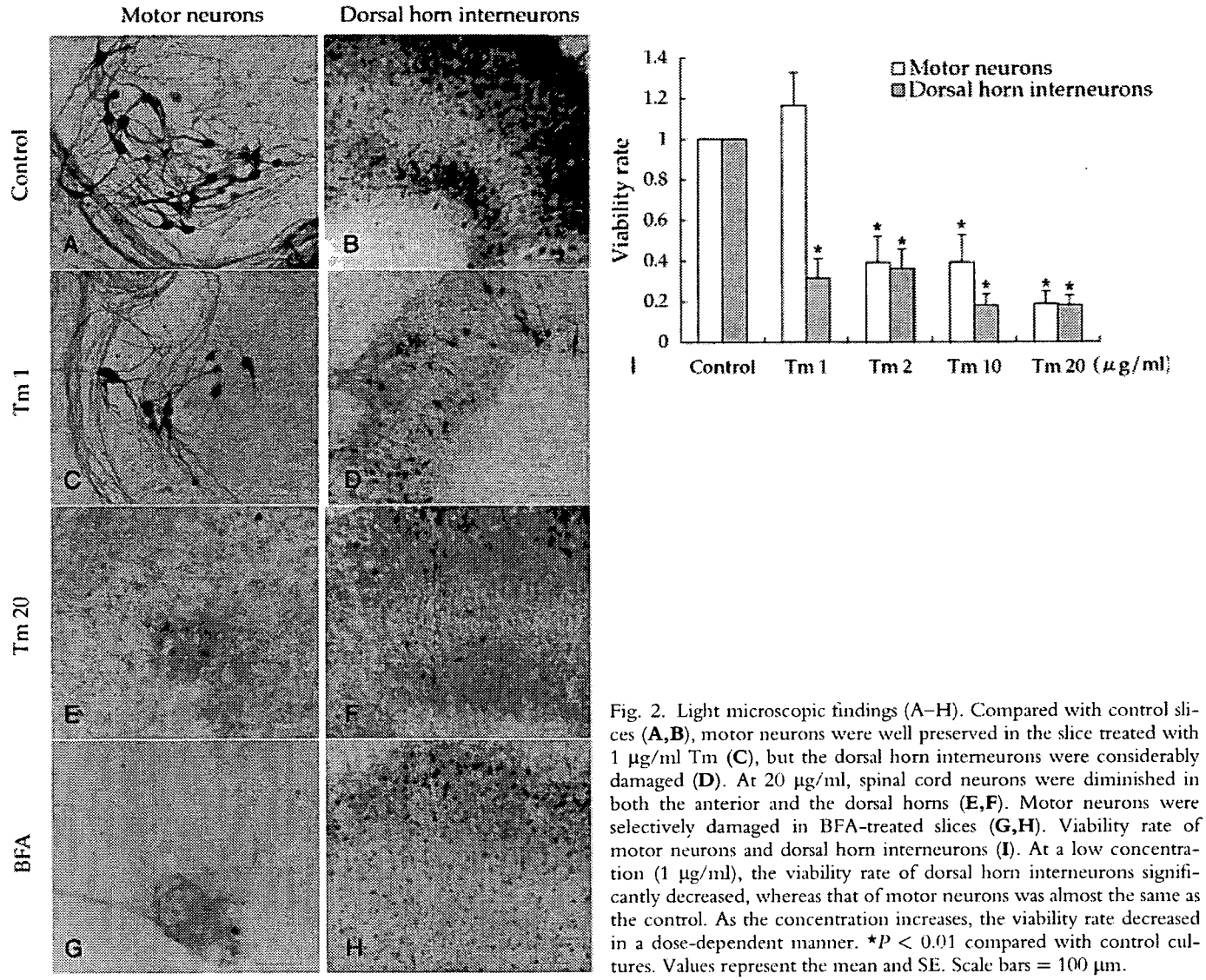

Fig. 2. Light microscopic findings (A–H). Compared with control slices (**A,B**), motor neurons were well preserved in the slice treated with 1 μg/ml Tm (**C**), but the dorsal horn interneurons were considerably damaged (**D**). At 20 μg/ml, spinal cord neurons were diminished in both the anterior and the dorsal horns (**E,F**). Motor neurons were selectively damaged in BFA-treated slices (**G,H**). Viability rate of motor neurons and dorsal horn interneurons (**I**). At a low concentration (1 μg/ml), the viability rate of dorsal horn interneurons significantly decreased, whereas that of motor neurons was almost the same as the control. As the concentration increases, the viability rate decreased in a dose-dependent manner. $*P < 0.01$ compared with control cultures. Values represent the mean and SE. Scale bars = 100 μm.

concentration of Tm was a high 20 μg/ml. The viability rate of motor neurons also increased with addition of PFT, but the difference was not statistically significant at any concentration of Tm tested.

Accumulation of p53 in the Dorsal Horn After Tm Treatment

Immunofluorescence analysis of slices cultured with Tm showed p53 immunoreactivity, which was considered to be p53-nuculear accumulation, in the dorsal horn area after double staining with antibodies for p53 and calretinin (Fig. 4). Calretinin-positive dorsal horn interneurons markedly decreased in Tm-treated slices and were not superimposed on p53-positive spots in a merged image. These findings suggest that the dorsal horn interneurons with nuclear translocation of p53 were too severely damaged to retain immunoreactivity for anticalretinin antibodies. In the anterior horns of Tm-treated slices, there was weak p53 staining of the cytosol of a motor neuron, but no definite evidence of nuclear accumulation. Control slices did not show any clear p53 staining in either the anterior horn or the dorsal horn. We also performed an immunofluorescence study with Hoechst 33258, but the background staining was too high for proper interpretation, and we could not determine whether apoptosis was involved in the neuronal death.

DISCUSSION

In the present study, Tm was shown to induce ER stress and spinal cord neurotoxicity, but it was not selective for motor neurons. Rather, dorsal horn interneurons were more vulnerable than motor neurons, which is inconsistent with the results of our previous study using

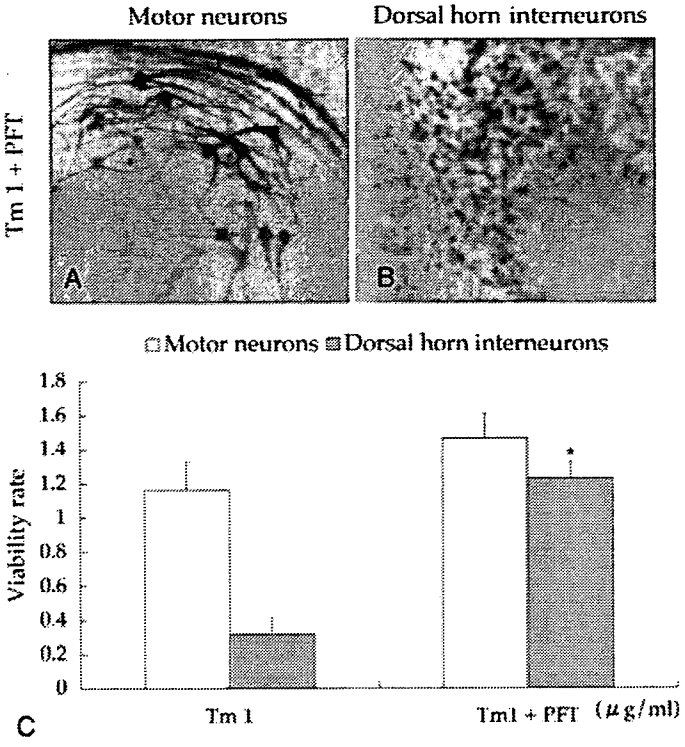

Fig. 3. Protective effect of PFT against neurotoxicity induced by 1 μg/ml Tm (**A,B**). The viability rate of the dorsal horn interneurons significantly increased in slices treated concomitantly with 1 μg/ml Tm and PFT (**C**). The viability rate of motor neurons did not significantly increase with PFT at any concentration of Tm (C). $*P < 0.01$. Values represent the mean and SE. Scale bars = 100 μm.

BFA as an ER stress inducer for cells in dissociated culture (Kikuchi et al., 2003). Although different experimental systems were used in the two studies, the discrepancy can be attributed to the different ER stress inducers, because BFA also tended to damage neurons in the anterior horn more severely than in the dorsal horn in our organotypic slice culture system.

Both Tm and BFA are potent ER stress inducers, and it is generally considered that they equally induce ER stress in several experimental systems (Nakagawa et al., 2000; Aoki et al., 2002; Shiraishi et al., 2005), but the mechanism causing ER stress is different. Tm inhibits protein N-linked glycosylation inside the ER, whereas BFA blocks protein transport from the ER to the Golgi apparatus. This difference in action can have various consequences, as we have shown in the present study. Even when both Tm and BFA exert the same effect on one cell type, their effects on another cell type might not always be the same (Ledesma et al., 2002).

In general, various kinds of stress acting on the ER cause the UPR, and, when cells cannot cope with the stress, apoptosis occurs via several signaling pathways. We used a p53 inhibitor to examine whether p53 was involved in ER-stress induced apoptosis, because there is accumulating evidence for the contribution of p53 to the stress-signaling pathways leading to neuronal death. A p53 inhibitor, PFT, was effective at protecting dorsal horn interneurons from Tm neurotoxicity in this study. In addition, immunofluorescence showed nuclear accumulation of p53 in the dorsal horns of slices treated with Tm. Thus, the induction of dorsal horn neuronal damage by Tm was shown to be p53 dependent.

p53 Is a well-known tumor suppressor gene product, and its antitumor activity is achieved primarily through the induction of apoptosis (Schmitt et al., 2002). The mechanisms by which p53 induces apoptosis are both transcription dependent and independent (Fridman and Lowe, 2003; Fig. 5). After activation, p53 translocates to the nucleus and initiates the transcription of various proapoptotic factors that include death receptors, Bcl-2 proteins such as Bax, the BH3-only proteins Bid and Noxa, and p53 up-regulated modulation of apoptosis (PUMA; Culmsee and Mattson, 2005). p53 Also accumulates in the cytoplasm, where it mediates mitochondrial outer membrane permeabilization through direct physical interaction with Bax in a transcription-independent manner (Chipuk et al., 2004). After the mitochondrial outer membrane permeabilization occurs, factors such as cytochrome c and apoptosis-inducing factor (AIF) are released to activate caspase-dependent and -independent cell death processes, respectively (Hong et al., 2004).

PFT is a synthetic, cell-permeable p53 inhibitor that mainly inhibits translocation of p53 into the nucleus (Culmsee and Mattson, 2005). PFT was originally isolated for its ability to reversibly block p53-dependent transcriptional activation and apoptosis (Komarov et al., 1999). It has been shown that PFT suppresses the transactivation of p53-responsive genes encoding p21, Mdm2, cyclin G, and Bax, and the antiapoptotic effect of PFT has been found to be p53-dependent (Gudkov and Komarova, 2005). Also, PFT lowers the nuclear, but not cytoplasmic, level of p53 protein after DNA damage (Komarov et al., 1999). Taken together, these observations suggest that the major mechanism by which PFT protects against apoptosis is the inhibition of p53 nuclear translocation (Fig. 5).

Our results suggest that p53 nuclear translocation plays the central role in the mechanism leading to Tm-induced death of dorsal horn interneurons, which provides strong support for those earlier reports. On the other hand, the viability rate of motor neurons did not significantly increase by PFT, and p53 nuclear accumulation was not found in the anterior horns of Tm-treated slices. These findings indicate that p53 nuclear translocation might not be primarily involved in Tm-induced motor neuronal death. A study using several tumor cell lines demonstrated that ER stress inhibited p53-mediated apoptosis through the increased cytoplasmic localization of p53 (Qu et al., 2004). This indicates that the actions of p53 may depend on the cell type and that motor neurons might have different mechanisms for coping with various cellular stresses compared with other neurons.

With regard to the mechanisms of Tm-induced dorsal horn interneuronal death, the downstream path-

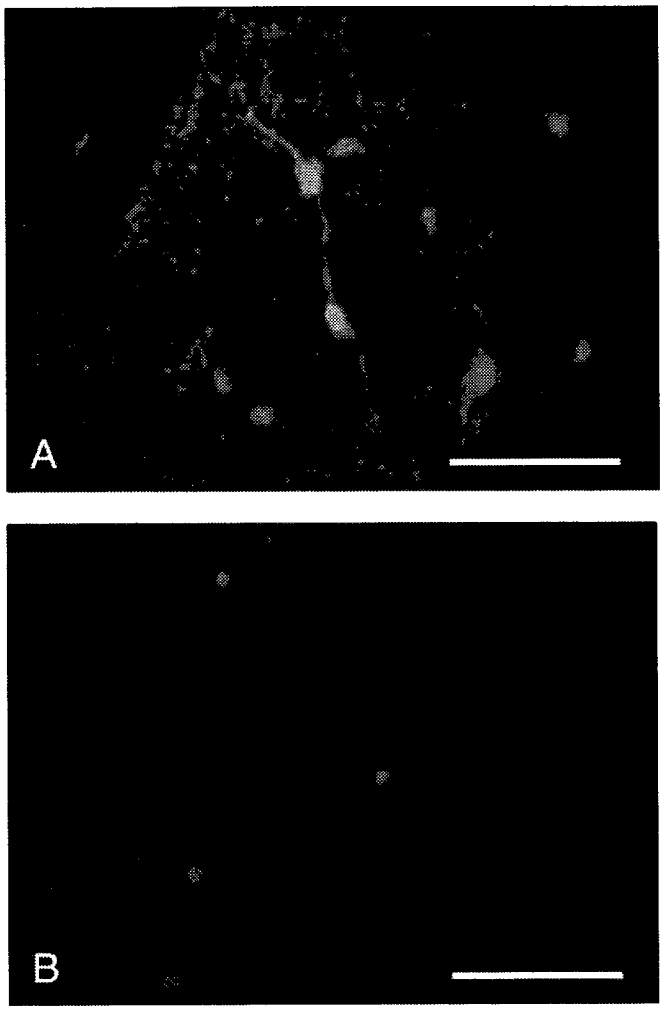

Fig. 4. Immunofluorescence micrographs of a dorsal horn doubly stained with anticalretinin antibody (**A**) and anti-p53 monoclonal antibody (**B**). Dorsal horn interneurons were severely damaged (A), and nuclear accumulation of p53 is seen in the dorsal horn of a slice treated with Tm (B). Control slices showed no p53 immunoreactivity in either the anterior horn or the dorsal horn (not shown). Scale bars = 100 μm.

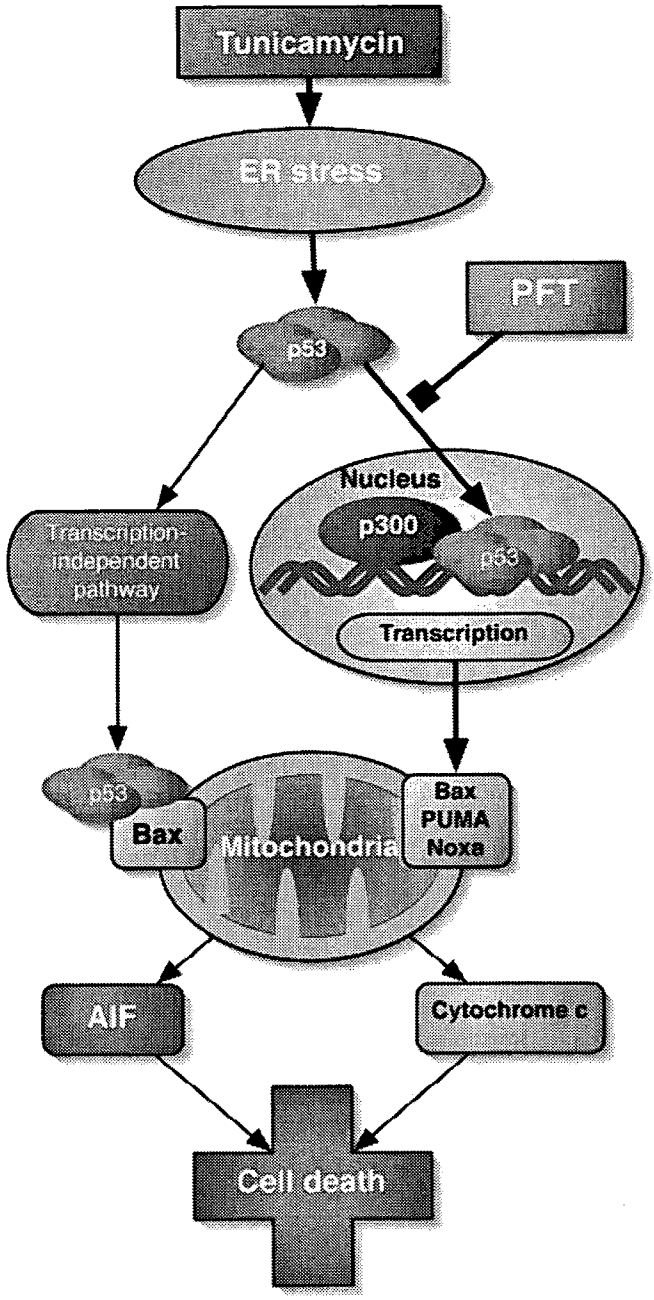

Fig. 5. Diagram of the pathways that may be involved in Tm-induced neuronal death. In the present study, PFT was significantly effective at ameliorating Tm-induced dorsal horn interneuronal toxicity, and nuclear accumulation of p53 was demonstrated by immunofluorescence, suggesting that the nuclear translocation of p53 was necessary for Tm to kill dorsal horn interneurons. Motor neurons may be damaged via different mechanisms, including a p53 transcription-independent pathway, because these cells were not effectively protected by PFT.

ways after the translocation of p53 to the nucleus have not been demonstrated in the present study. As well as the contribution of caspase cascade to this process, the involvement of apoptosis in the dorsal horn interneuronal death itself remains to be clarified. We are working on these issues to reveal the network of the pathways leading to ER-stress-induced neuronal death.

In conclusion, the present study has shown that dorsal horn interneurons were more vulnerable to Tm-induced neurotoxicity than motor neurons in organotypic slice cultures of rat spinal cord and that this toxicity was effectively attenuated by PFT, suggesting the involvement of p53 in Tm-induced dorsal horn interneuronal death. We could not detect a significant protective effect of PFT against motor neuronal death, but the difference between dorsal horn interneurons and motor neurons may be a clue to a better understanding of the stress-response pathways. Moreover, a better understanding of the pathways involved might allow p53 inhibitors to be used in the treatment of spinal cord conditions,

such as ischemia and injury, or demyelinating and neurodegenerative diseases, including ALS.

REFERENCES

Aoki S, Su Q, Li H, Nishikawa K, Ayukawa K, Hara Y, Namikawa K, Kiryu-Seo S, Kiyama H, Wada K. 2002. Identification of an axotomy-induced glycosylated protein, AIGP1, possibly involved in cell death triggered by endoplasmic reticulum-Golgi stress. J Neurosci 22:10751–10760.

Chipuk JE, Kuwana T, Bouchier-Hayes L, Droin NM, Newmeyer DD, Schuler M, Green DR. 2004. Direct activation of Bax by p53 mediates mitochondrial membrane permeabilization and apoptosis. Science 303: 1010–1014.

Culmsee C, Mattson MP. 2005. p53 In neuronal apoptosis. Biochem Biophys Res Commun 331:761–777.

DeGracia DJ, Montie HL. 2004. Cerebral ischemia and the unfolded protein response. J Neurochem 91:1–8.

Fridman JS, Lowe SW. 2003. Control of apoptosis by p53. Oncogene 22:9030–9040.

Fujita Y, Okamoto K. 2005. Golgi apparatus of the motor neurons in patients with amyotrophic lateral sclerosis and in mice models of amyotrophic lateral sclerosis. Neuropathology 25:388–394.

Gudkov AV, Komarova EA. 2005. Prospective therapeutic applications of p53 inhibitors. Biochem Biophys Res Commun 331:726–736.

Hervias I, Beal MF, Manfredi G. 2005. Mitochondrial dysfunction and amyotrophic lateral sclerosis. Muscle Nerve [E-pub ahead of print].

Hetz C, Russelakis-Carneiro M, Maundrell K, Castilla J, Soto C. 2003. Caspase-12 and endoplasmic reticulum stress mediate neurotoxicity of pathological prion protein. EMBO J 22:5435–5445.

Hong SJ, Dawson TM, Dawson VL. 2004. Nuclear and mitochondrial conversations in cell death: PARP-1 and AIF signaling. Trends Pharmacol Sci 25:259–264.

Katayama T, Imaizumi K, Manabe T, Hitomi J, Kudo T, Tohyama M. 2004. Induction of neuronal death by ER stress in Alzheimer's disease. J Chem Neuroanat 28:67–78.

Kaufman RJ. 1999. Stress signaling from the lumen of the endoplasmic reticulum: coordination of gene transcriptional and translational controls. Genes Dev 13:1211–1233.

Kheradpezhouh M, Shavali S, Ebadi M. 2003. Salsolinol causing Parkinsonism activates endoplasmic reticulum-stress signaling pathways in human dopaminergic SK-N-SH cells. Neurosignals 12:315–324.

Kikuchi S, Shinpo K, Takeuchi M, Tsuji S, Yabe I, Niino M, Tashiro K. 2002. Effect of geranylgeranylaceton on cellular damage induced by proteasome inhibition in cultured spinal neurons. J Neurosci Res 69: 373–381.

Kikuchi S, Shinpo K, Tsuji S, Yabe I, Niino M, Tashiro K. 2003. Brefeldin A-induced neurotoxicity in cultured spinal cord neurons. J Neurosci Res 71:591–599.

Komarov PG, Komarova EA, Kondratov RV, Christov-Tselkov K, Coon JS, Chernov MV, Gudkov AV. 1999. A chemical inhibitor of p53 that protects mice from the side effects of cancer therapy. Science 285:1733–1737.

Ledesma MD, Galvan C, Hellias B, Dotti C, Jensen PH. 2002. Astrocytic but not neuronal increased expression and redistribution of parkin during unfolded protein stress. J Neurochem 83:1431–1440.

Liu CY, Kaufman RJ. 2003. The unfolded protein response. J Cell Sci 116:1861–1862.

Nakagawa T, Zhu H, Morishima N, Li E, Xu J, Yankner BA, Yuan J. 2000. Caspase-12 mediates endoplasmic-reticulum-specific apoptosis and cytotoxicity by amyloid-beta. Nature 403:98–103.

Nishitoh H, Matsuzawa A, Tobiume K, Saegusa K, Takeda K, Inoue K, Hori S, Kakizuka A, Ichijo H. 2002. ASK1 is essential for endoplasmic reticulum stress-induced neuronal cell death triggered by expanded polyglutamine repeats. Genes Dev 16:1345–1355.

Paschen W, Frandsen A. 2001. Endoplasmic reticulum dysfunction—a common denominator for cell injury in acute and degenerative diseases of the brain? J Neurochem 79:719–725.

Paschen W, Mengesdorf T. 2005. Endoplasmic reticulum stress response and neurodegeneration. Cell Calcium 38:409–415.

Qu L, Huang S, Baltzis D, Rivas-Estilla AM, Pluquet O, Hatzoglou M, Koumenis C, Taya Y, Yoshimura A, Koromilas AE. 2004. Endoplasmic reticulum stress induces p53 cytoplasmic localization and prevents p53-dependent apoptosis by a pathway involving glycogen synthase kinase-3beta. Genes Dev 18:261–277.

Rosen DR, Siddique T, Patterson D, Figlewicz DA, Sapp P, Hentati A, Donaldson D, Goto J, O'Regan JP, Deng HX, Rahmani Z, Krizus A, McKenna-Yasek D, Cayabyab A, Gaston SM, Berger R, Tanzi RE, Halperin JJ, Herzfeldt B, Van den Bergh R, Hung WY, Bird T, Deng G, Mulder DW, Smyth C, Laing NG, Soriano E, Pericak-Vance MA, Haines J, Rouleau GA, Gusella JS, Horvitz HR, Brown RH Jr. 1993. Mutations in Cu/Zn superoxide dismutase gene are associated with familial amyotrophic lateral sclerosis. Nature 362:59–62.

Schmitt CA, Fridman JS, Yang M, Baranov E, Hoffman RM, Lowe SW. 2002. Dissecting p53 tumor suppressor functions in vivo. Cancer Cell 1:289–298.

Shen X, Zhang K, Kaufman RJ. 2004. The unfolded protein response—a stress signaling pathway of the endoplasmic reticulum. J Chem Neuroanat 28:79–92.

Shiraishi T, Yoshida T, Nakata S, Horinaka M, Wakada M, Mizutani Y, Miki T, Sakai T. 2005. Tunicamycin enhances tumor necrosis factor-related apoptosis-inducing ligand-induced apoptosis in human prostate cancer cells. Cancer Res 65:6364–6370.

Swanton E, Holland A, High S, Woodman P. 2005. Disease-associated mutations cause premature oligomerization of myelin proteolipid protein in the endoplasmic reticulum. Proc Natl Acad Sci U S A 102: 4342–4347.

Takahashi R, Imai Y. 2003. Pael receptor, endoplasmic reticulum stress, and Parkinson's disease. J Neurol 250(Suppl 3):III/25–III/29.

Takahashi R, Imai Y, Hattori N, Mizuno Y. 2003. Parkin and endoplasmic reticulum stress. Ann NY Acad Sci 991:101–106.

Tessitore A, Martin MP, Sano R, Ma Y, Mann L, Ingrassia A, Laywell ED, Steindler DA, Hendershot LM, d'Azzo A. 2004. GM1-ganglioside-mediated activation of the unfolded protein response causes neuronal death in a neurodegenerative gangliosidosis. Mol Cell 15:753–766.

Tobisawa S, Hozumi Y, Arawaka S, Koyama S, Wada M, Nagai M, Aoki M, Itoyama Y, Goto K, Kato T. 2003. Mutant SOD1 linked to familial amyotrophic lateral sclerosis, but not wild-type SOD1, induces ER stress in COS7 cells and transgenic mice. Biochem Biophys Res Commun 303:496–503.

Tsuji S, Kikuchi S, Shinpo K, Tashiro J, Kishimoto R, Yabe I, Yamagishi S, Takeuchi M, Sasaki H. 2005. Proteasome inhibition induces selective motor neuron death in organotypic slice cultures. J Neurosci Res 82:443–451.

Vattemi G, Engel WK, McFerrin J, Askanas V. 2004. Endoplasmic reticulum stress and unfolded protein response in inclusion body myositis muscle. Am J Pathol 164:1–7.

Wootz H, Hansson I, Korhonen L, Napankangas U, Lindholm D. 2004. Caspase-12 cleavage and increased oxidative stress during motoneuron degeneration in transgenic mouse model of ALS. Biochem Biophys Res Commun 322:281–286.

Zhang K, Kaufman RJ. 2006. The unfolded protein response: a stress signaling pathway critical for health and disease. Neurology 66(Suppl 1): S102–S109.

Journal of Neuroscience Research 82:443–451 (2005)

Proteasome Inhibition Induces Selective Motor Neuron Death in Organotypic Slice Cultures

Sachiko Tsuji,[1]* Seiji Kikuchi,[1] Kazuyoshi Shinpo,[2] Jun Tashiro,[1] Riichiro Kishimoto,[1] Ichiro Yabe,[1] Shoichi Yamagishi,[3] Masayoshi Takeuchi,[4] and Hidenao Sasaki[1]

[1]Department of Neurology, Hokkaido University Graduate School of Medicine, Kita-ku, Sapporo, Japan
[2]Nishimaruyama Hospital, Chuo-ku, Sapporo, Japan
[3]Department of Internal Medicine III, Kurume University School of Medicine, Kurume, Japan
[4]Department of Pathophysiological Science, Faculty of Pharmaceutical Science, Hokuriku University, Kanazawa, Japan

A dysfunctional ubiquitin-proteasome system recently has been proposed to play a role in the pathogenesis of neurodegenerative diseases, including amyotrophic lateral sclerosis (ALS). We have shown previously that spinal motor neurons are more vulnerable to proteasome inhibition-induced neurotoxicity, using a dissociated culture system. To confirm this toxicity, we used organotypic slice cultures from rat neonatal spinal cords, which conserve the structure of the spinal cord in a horizontal plane, enabling us to identify motor neurons more accurately than in dissociated cultures. Furthermore, such easy identifications make it possible to follow up the course of the degeneration of motor neurons. When a specific proteasome inhibitor, lactacystin (5 μM), was applied to slice cultures, proteasome activity of a whole slice was suppressed below 30% of control. Motor neurons were selectively damaged, especially in neurites, with the increase of phosphorylated neurofilaments. They were eventually lost in a dose-dependent manner (1 μM, $P < 0.05$; 5 μM, $P < 0.01$). The low capacity of Ca^{2+} buffering is believed to be one of the factors of selectivity for damaged motor neurons in ALS. In our system, negative staining of Ca^{2+}-binding proteins supported this notion. An intracellular Ca^{2+} chelator, BAPTA-AM (10 μM), exerted a significant protective effect when it was applied with lactacystin simultaneously ($P < 0.01$). We postulate that proteasome inhibition is an excellent model for studying the mechanisms underlying selective motor neuron death and searching for new therapeutic strategies in the treatment of ALS.

Key words: amyotrophic lateral sclerosis; motor neuron; proteasome; calcium

Amyotrophic lateral sclerosis (ALS) is a fatal neurodegenerative disease causing progressive muscular atrophy and weakness. Riruzole is the only medicine clinically approved to delay the progression, but its effect is unsatisfactory. The disease in most patients is sporadic and of unknown cause, but about 10% of the cases are familial. In 1994, mutations of copper/zinc superoxide dismutase (SOD1) (ALS1) were reported to cause a dominantly inherited ALS that closely resembles the sporadic form (Rosen et al., 1993). Since then, more than 110 kinds of SOD1 mutations have been reported (www.alsod.org). Because SOD1-knockout mice did not show any phenotypes of motor neuron diseases (Reaume et al., 1996) whereas mutant SOD1 transgenic mice reproduced clinical signs and pathologies affecting motor neurons (Gurney et al., 1994), the mechanism by which SOD1-mutations cause motor neuron degeneration not should not be a loss of function, but rather an adverse gain of function. Some attractive hypotheses, about excitotoxicity, oxidative damage, abnormal accumulation of phosphorylated neurofilaments, mitochondrial dysfunction, and impairment of the ubiquitin-proteasome system (UPS) have been discussed (Bruijn et al., 2004).

Protein accumulation is a common and crucial pathological feature of neurodegenerative diseases that could mean impairment of protein degradation (Ciechanover and Brundin, 2003). In ALS, skein-like inclusions (SLIs), round hyaline inclusions (RHIs), and Bunina bodies are the specific markers of the disease in sporadic form, and Lewy body-like hyaline inclusions (LBHIs) are in ALS1 (Wood et al., 2003). SLIs, RHIs and LBHIs frequently contain ubiquitin, a signal of degradation in the 26S-proteasome. UPS plays a major role in cell survival by degradation of proteins in a relatively

Contract grant sponsor: Ministry of Health, Labor, and Welfare of Japan.

*Correspondence to: Dr. Sachiko Tsuji, Department of Neurology, Hokkaido University Graduate School of Medicine, North 15, West 7, Kita-ku, Sapporo 060-8648, Japan. E-mail: tujitti@jb3.so-net.ne.jp

Received 15 July 2005; Revised 23 August 2005; Accepted 26 August 2005

Published online 18 October 2005 in Wiley InterScience (www.interscience.wiley.com). DOI: 10.1002/jnr.20665

short time, which regulates various functions such as signal transduction, cell cycle, and synaptic modulation (Korhonen and Lindholm, 2004). The pathologies of ubiquitin-positive inclusion might suggest the involvement of UPS in ALS.

In $SOD1^{G93A}$ transgenic mice, which are hindlimb-onset, the focal decrease of proteasome activity in lumber spinal cords preceded the clinical motor symptom (Kabashi et al., 2004). It is also reported that $SOD1^{G93A}$-transfected cells fell into proteasome dysfunction and motor neurons were specifically vulnerable in primary culture systems (Kikuchi et al., 2002; Urushitani et al., 2002). There is a report examining protease activity in ALS patients, however, which concluded that there were no significant changes in the cytoplasmic protease activity of the spinal cords (Shaw et al., 1996). In a study with slice cultures of mouse spinal cords, no specific vulnerability of motor neurons was seen compared to neurons in the posterior horns (Vlug and Jaarsma, 2004).

To confirm whether motor neurons are vulnerable to proteasomal dysfunction, we investigated the organotypic slice cultures of neonatal rat spinal cords exposed to the specific proteasome inhibitor, lactacystin. Proteasome inhibition induced severe degeneration of motor neurons but the minimum change in the posterior horns and the difference was considered to be due to the low buffering ability of intracellular Ca^{2+} in motor neurons.

MATERIALS AND METHODS

Materials

The following reagents were used in these experiments: SMI-31, -32, and -34 (Sternberger Monoclonals Incorporated, Lutherville, MD); anti-calretinin antibody and anti-calbindin D-28K antibody (Chemicon, Temecula, CA); Eagle's MEM and glutamine (Nissui, Tokyo, Japan); fetal bovine serum (FBS) and Gey's balanced solution (Sigma, St. Louis, MO); Hank's balanced salt solution (HBSS; Gibco BRL, Grand Island, NY); lactacystin, epoxomicin, and MCA-conjugated protease substrates (Peptide Institute, Osaka, Japan); 6-cyano-7-nitroquinoxaline-2, 3-dione (CNQX) and (+)-MK-801 hydrogen maleate (Research Biochemicals International, Natick, MA); ifenprodil tartrate salt and nimodipine (Sigma); BAPTA-AM (Dojindo, Kumamoto, Japan); peroxidase anti-mouse IgG (H+L) and anti-rabbit IgG antibodies (Vector, Burlingame, CA), Alexa Fluor 488 goat anti-mouse IgG, Alexa Fluor 568 goat anti-rabbit IgG, Zenon Alexa Fluor 488 mouse IgG1 labeling kit (Molecular Probes, Eugene, OR); and rhodamine-conjugated anti-mouse Igs (Tagoimmunologicals, Camarillo, CA).

Organotypic Slice Cultures

These procedures were carried out under the approval of the animal care and use committee of Hokkaido University School of Medicine. Organotypic slice cultures were prepared as described previously (Stoppini et al., 1991). Briefly, after deep anesthesia with ketamine, neonatal Day 6 Sprague-Dawley rats were decapitated and their lumber spinal cords were removed. Nerve roots and excessive tissues were removed in a cooled Gey's balanced salt solution containing 6.5 mg/ml of glucose. Spinal cords were then cut into 400-μm slices with a McIlwain tissue chopper (Mickle Laboratory Engineering Co. Ltd., Gomshall, Surrey, UK). Four slices were put onto a membrane insert (Millicell-CM; Millipore, Bedford, MA) and placed in a 6-well culture dish containing 1 ml of culture medium consisting of 50% Eagle's MEM, 25% HBSS, 25% horse serum, 6.4 mg/ml of glucose, and 2 mM L-glutamine. The slices were incubated at 37°C in a 5% CO_2 incubator and the culture medium was changed twice a week. All cultures were used in the experiments after 10 days in vitro.

Immunohistochemistry and Immunofluorescence

For the labeling of neurons in spinal cord slices, the cultures were fixed with 4% paraformaldehyde for 1 hr, rinsed with phosphate-buffered saline (PBS) and, after blocking, stained overnight at 4°C with SMI-32 (1:2,500) or the polyclonal antibody against calretinin (1:5,000), diluted in PBS containing 0.3% Triton X-100 and 0.2% bovine albumin. After several washings with PBS containing 0.3% Triton X-100, the cultures were incubated with a secondary antibody (1:250) for 3 hr and visualized with diaminobenzidine tetrahydrochloride (DAB).

For immunofluorescence analysis, the fixation and primary antibody procedures were the same as described for immunohistochemistry. Secondary antibodies (1:100) were incubated for 1 hr. When two kinds of mouse-derived primary antibodies are used in the same staining, the Zenon mouse IgG labeling kit is useful to distinguish between them. Using the Zenon mouse IgG labeling kit, Alexa Fluor 488-labeled goat Fab fragments against mouse IgG Fc fragments can form complexes with mouse-derived primary antibodies before their application on slices, simplifying procedures that use multiple mouse-derived antibodies. After SMI-31 (or -34) and the secondary antibody, Alexa Fluor 568-tagged anti-mouse IgG, were applied, SMI-32 that had been labeled with a Zenon One kit beforehand was incubated for 90 min. Photographs were taken using a fluoroscope with a CCD camera (Nikon, Tokyo, Japan) in black and white at first, and colored with software Image-Pro 2 (Media Cybernetics, Silver Springs, MD) later. Some pictures were also taken with confocal microscopy (MRC-1024; Bio-Rad).

Measurement of Proteasome Activity

Proteasome activity was assayed with MCA-binding substrates producing AMC when the substrates were cleaved. An increase of AMC can be monitored photometrically at 370 nm. A lysate for one experiment was made from four slices on a membrane. They were crushed in an ice-cooled buffer (20 mM Tris, 20 mM NaCl, 1 μM EDTA, and 5 mM 2-mercaptoethanol; pH 7.6) and divided into 50-μL aliquots. Equivalent doses of a proteolysis buffer (4 mM ATP, 10 mM $MgCl_2$, and 8 mM dithiothreitol) containing 100 μM AMC-binding substrate (Boc-LRR-AMC, Suc-LLVY-AMC, Z-LLE, substrates as trypsin-like, chymotrypsin-like, peptidylglutamyl-peptide hydrolytic proteolytic protease) were added. After incubation at 37°C for 30 min, an absorbance of 370-nm wavelength was measured with a UV spectrophotometer. Lysates without any

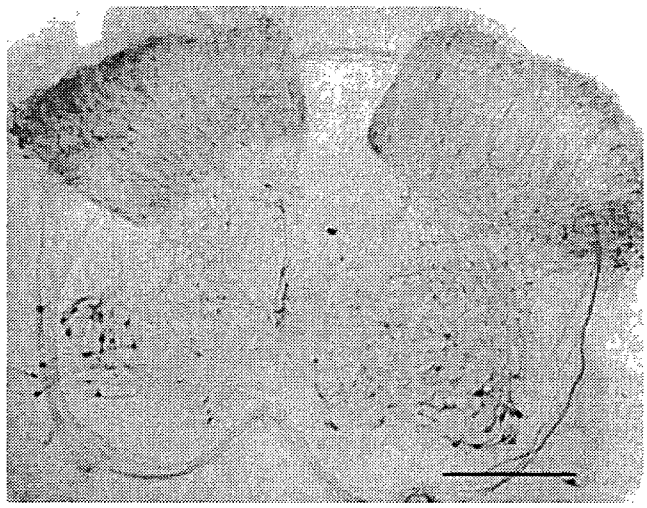

Fig. 1. Immunohistochemistry of whole slice culture with SMI-32. Large, strongly SMI-32-positive motor neurons gathered in lateral anterior horns. Scale bar = 400 μm.

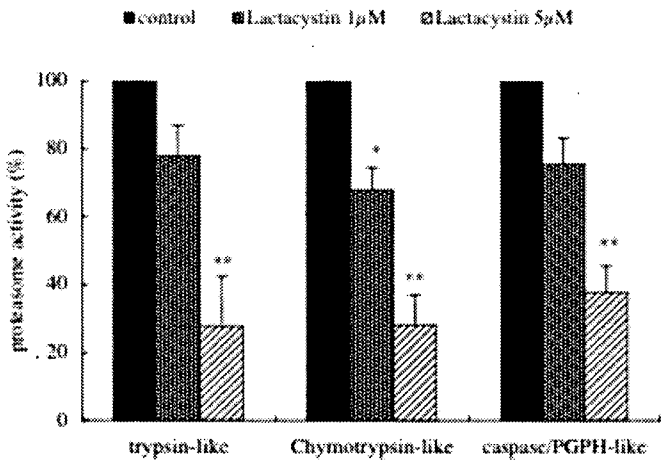

Fig. 2. Three kinds of protease activities of proteasome were significantly inhibited in a dose-dependent manner after a 3-hr exposure to lactacystin. $^{*}P < 0.05$, $^{**}P < 0.01$.

substrates were used for a reference. Data were corrected with a protein amount and represented as a rate of the non-lactacystin-treated sample. The protein concentration was measured with a protein assay kit using Bradford's method (Bio-Rad protein assay kit; Bio-Rad, Tokyo, Japan).

Experimental Treatment of Organotypic Slices and Quantification of Cell Death

The organotypic slices were exposed to two kinds of proteasome inhibitor, lactacystin and epoxomicin, in the culture medium at various concentrations (lactacystin, 0.5–5 μM; epoxomicin, 10–50 nM) for 72 hr in a 5% CO_2 incubator maintained at 37°C. To study the involvement of excitotoxicity in the proteasome inhibition-induced effects, glutamate receptor antagonists were used. These included the non-competitive *N*-methyl-D-aspartate (NMDA) receptor blocker,

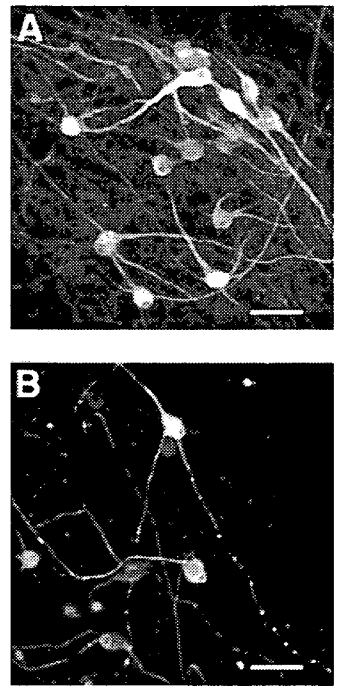

Fig. 3. Immunofluorescence with SMI-32. **A:** Motor neurons without lactacystin have thick and long neurites. **B:** After 36 hr of exposure to lactacystin, fragmentation of neurites started.

MK-801 (10 μM), the specific blocker of the NMDA receptor containing an NR2B subunit, ifenprodil (10 μM), and the competitive α-amino-3-hydroxy-5-methylisoxasole-4-propionate (AMPA)/kainate receptor blocker, CNQX (50 μM). These inhibitors were coincubated with lactacystin for 72 hr in the culture medium. To examine the effect of calcium activity, the intracellular calcium chelator BAPTA-AM (10 μM), and an L-type calcium channel blocker, nimodipine (20 μM), were coadministered with lactacystin for 72 hr.

Statistical Analysis

All data presented in this study are representative of at least four cultured slices of every experiment, repeated three times independently. Statistical analysis was carried out using analysis of variance (ANOVA), followed by the post-hoc test (Tukey's method) with the Excel add-in software, Statcel2.

RESULTS

Early Change of Motor Neurons by Proteasome Inhibition

The organotypic spinal cord culture was established referring to past articles (Stoppini et al., 1991; Bergold et al., 1997). A horizontal structure was preserved and many motor neurons were detected in the anterior horns in SMI-32 stains (Fig. 1). Some neurons in the dorsal horns were as large as motor neurons, which could be misidentified as motor neurons if their location were unavailable, as in a dissociate culture. We defined surviv-